Computers and Mathematics with Applications 61 (2011) 1431–1441

Contents lists available at ScienceDirect

Computers and Mathematics with Applications

journal homepage: www.elsevier.com/locate/camwa

Convection from an inverted cone in a porous medium with cross-diffusion effects

F.G. Awad [a], P. Sibanda [a,*], S.S. Motsa [b], O.D. Makinde [c]

[a] School of Mathematical Sciences, University of KwaZulu-Natal, Private Bag X01, Scottsville 3209, Pietermaritzburg, South Africa

[b] Department of Mathematics, University of Swaziland, Private Bag 4, Kwaluseni, Swaziland

[c] Faculty of Engineering, Cape Peninsula University of Technology, P. O. Box 652, Cape Town 8000, South Africa

ARTICLE INFO

Article history:
Received 7 October 2010
Received in revised form 11 January 2011
Accepted 11 January 2011

Keywords:
Inverted cone
Cross-diffusion
Numerical solution
Linearisation method

ABSTRACT

In this study convection from an inverted cone in a porous medium with cross-diffusion is studied numerically. Diffusion-thermo and thermo-diffusion effects are assumed to be significant. The governing equations are transformed into nonlinear ordinary differential equations and then solved numerically using a shooting method together with a sixth order Runge–Kutta method. Verification of the accuracy and correctness of the results is achieved by solving the equations using an independent linearisation method. The effects of the Dufour and the Soret parameters are investigated. The results for the skin friction, Nusselt number and the Sherwood number are presented graphically and in tabular form.

1. Introduction

The study of combined heat and mass transfer on a surface embedded in saturated porous media has attracted considerable attention in recent decades due to many engineering applications such as in the design of pebble-bed nuclear reactors, ceramic processing, crude oil drilling, compact heat exchangers, etc. Studies on natural convection flows have been carried out on vertical, inclined and horizontal surfaces in a porous medium by, among others, Cheng [1,2], Nield and Bejan [3] and Ingham and Pop [4]. Na and Chiou [5] presented the problem of laminar natural convection of Newtonian fluids over a frustum of a cone. Lai [6] investigated the heat and mass transfer by natural convection from a horizontal line source in saturated porous medium. Natural convection over a vertical wavy cone has been investigated by Pop and Na [7]. Nakyam and Hussain [8] studied the combined heat and mass transfer by natural convection in a porous medium by integral methods. Cheng [9] examined the effects of a magnetic field on heat and mass transfer by natural convection from a vertical surface in porous media by an integral approach. Chamkha and Khaled [10] studied the hydromagnetic heat and mass transfer by mixed convection from a vertical plate embedded in a uniform porous medium. Chamkha [11] investigated the coupled heat and mass transfer by natural convection of Newtonian fluids about a truncated cone in the presence of magnetic field and radiation effects and Yih [12] examined the effect of radiation in convective flow over a cone. Cheng [13] used an integral approach to study the heat and mass transfer by natural convection from truncated cones in porous media with variable wall temperature and concentration. Cheng [14] investigated the natural convection and mass transfer near a vertical truncated cone with wall heating and convection in a porous medium saturated with non-Newtonian power-law fluids. Khanafer and Vafai [15] studied the double-diffusive convection in a lid-driven enclosure filled with a fluid-saturated porous medium. Kumer et al. [16] investigated the effects of thermal stratification on double-diffusive natural convection in a vertical porous enclosure.

* Corresponding author. Tel.: +27 33 260 5626; fax: +27 33 260 5648.
E-mail addresses: 208529540@ukzn.ac.za (F.G. Awad), sibandap@ukzn.ac.za (P. Sibanda), sandilemotsa@gmail.com (S.S. Motsa), makinded@cput.ac.za (O.D. Makinde).

0898-1221/$ – see front matter © 2011 Elsevier Ltd. All rights reserved.
doi:10.1016/j.camwa.2011.01.015

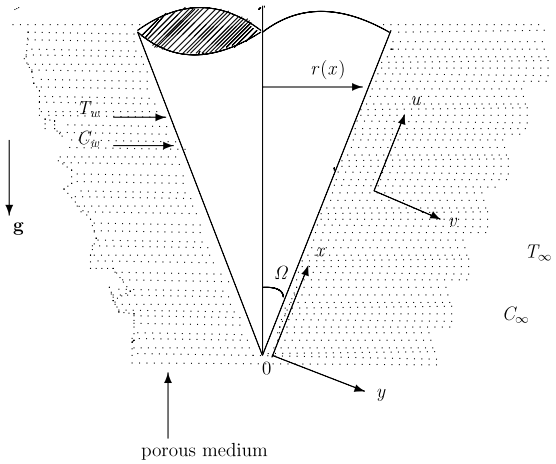

Fig. 1. Schematic sketch of the vertical cone.

In double-diffusive convection the density of the fluid mixture depends on the temperature, the concentration and on the pressure. In this case there is direct coupling of the conservation equations and, as has been shown in previous studies (see, for example, [17–19]), the Soret mass flux and Dufour energy flux have significant effect on heat and mass transfer rates. Thermal-diffusion and diffusion-thermo effects on mixed free and forced convection in boundary layer flow in clear fluids with temperature dependent viscosity have been studied by among others, Kafoussias and Williams [20], Chamkha and Ben-Nakhi [21], Sovran et al. [22] and Postelnicu [23]. Sohouli et al. [24] applied the homotopy analysis method to study natural convection of Darcian fluid about a vertical cone embedded in porous media with a prescribed surface heat flux to get the analytical solutions of the governing nonlinear equations.

In this work we determine numerical solutions of the nonlinear equations that govern convection about a vertical cone in the presence of Dufour energy flux and Soret mass effects. Cheng [14] studied the Dufour and Soret effects on the steady boundary layer flow due to natural convection heat and mass transfer over a downward-pointing vertical cone embedded in a porous medium saturated with Newtonian fluids with constant wall temperature and concentration. The study extends the earlier work by Sohouli et al. [24] to include Dufour and Soret effects.

In this work we apply a shooting technique together with a sixth order Runge–Kutta method (see [25,26]) to solve the resulting nonlinear equations numerically. The accuracy of the results is verified by further solving the governing equations using a recent linearisation; see Makukula et al. [27,28]. We show by comparison with numerical results that this linearisation method is accurate and converges rapidly to the true solution.

2. Mathematical formulation

Consider an inverted cone in a porous medium with semi-angle Ω. We take the origin of the coordinate system to be at the vertex of the cone, the x-axis is the coordinate along the surface of the cone and y is the coordinate normal to the surface of the cone as shown in Fig. 1.

The surface of the cone is subject to a non-uniform temperature $T_w > T_\infty$ where T_∞ is the temperature far from the surface of the cone. The solute concentration varies from C_w on the surface of the inverted cone to a lower concentration C_∞ in the ambient fluid. Under the Boussinesq approximation, the governing equations can be written as:

$$\frac{\partial}{\partial x}(ru) + \frac{\partial}{\partial y}(rv) = 0 \tag{1}$$

$$u\frac{\partial u}{\partial x} + v\frac{\partial u}{y} = \nu\frac{\partial^2 u}{\partial y^2} - \frac{\nu}{K}u + \rho g\beta\cos\Omega(T - T_\infty) + \rho g\beta^*\cos\Omega(C - C_\infty), \tag{2}$$

$$u\frac{\partial T}{\partial x} + v\frac{\partial T}{\partial y} = \alpha\frac{\partial^2 T}{\partial y^2} + \frac{Dk}{c_s c_p}\frac{\partial^2 C}{\partial y^2}, \tag{3}$$

$$u\frac{\partial C}{\partial x} + v\frac{\partial C}{\partial y} = D\frac{\partial^2 C}{\partial y^2} + \frac{Dk}{c_s c_p}\frac{\partial^2 T}{\partial y^2}, \tag{4}$$

where for a thin boundary layer $r = x\sin\Omega$, u and v are the velocity components in the x and y directions respectively, g is the acceleration due to gravity, ρ is the fluid density, K is the permeability, ν is kinematic viscosity of the fluid, respectively, β and β^* are the thermal expansion and the concentration expansion coefficients respectively, α and D are the thermal and mass diffusivities of the saturated porous medium, k is the thermal-diffusion ratio, c_p is the specific heat at constant pressure, and c_s is the concentration susceptibility.

We assume that either a power-law of temperature and concentration or a power-law of heat and mass flux is prescribed on the frustum. Accordingly, the boundary conditions are

$$u = 0, \qquad v = 0, \qquad T = T_w = T_\infty + Ax^\lambda, \qquad C = C_w = C_\infty + Bx^\lambda \quad \text{on } y = 0,\ x \geq 0 \tag{5}$$

$$u = 0, \qquad T = T_\infty, \qquad C = C_\infty \quad \text{as } y \to \infty, \tag{6}$$

where $A, B > 0$ are constants and λ is the power-law index. The subscripts w and ∞ refer to the cone surface and ambient conditions respectively. It is convenient to introduce the stream function ψ defined by:

$$u = \frac{1}{r}\frac{\partial \psi}{\partial y} \quad \text{and} \quad v = -\frac{1}{r}\frac{\partial \psi}{\partial x}, \tag{7}$$

and apply the following transformations

$$\eta = \frac{y}{x} Gr_x^{\frac{1}{4}}, \qquad \psi = \nu r Gr_x^{\frac{1}{4}} f(\eta), \qquad u = \frac{\nu}{x} Gr_x^{\frac{1}{2}} f', \qquad v = \frac{\nu}{x} Gr_x^{\frac{1}{4}} (\eta f' - f),$$

$$\theta(\eta) = \frac{T - T_\infty}{T_w - T_\infty}, \qquad \phi(\eta) = \frac{C - C_\infty}{C_w - C_\infty}, \tag{8}$$

where Gr_x is the local Rayleigh number defined by:

$$Gr_x = \frac{\rho g \beta \cos \Omega (T_w - T_\infty) x^3}{\nu^2}. \tag{9}$$

Substituting the transformations (8) into Eqs. (1)–(6) we obtain the following ordinary differential equations:

$$f''' + \left(\frac{\lambda + 7}{4}\right) f f'' - \left(\frac{\lambda + 1}{2}\right) f'^2 - \Lambda f' + \theta + N_1 \phi = 0, \tag{10}$$

$$\theta'' + D_f \phi'' + \Pr \left(\frac{\lambda + 7}{4}\right) f \theta' - \Pr \lambda f' \theta = 0, \tag{11}$$

$$\phi'' + S_r \theta'' + \mathrm{Sc} \left(\frac{\lambda + 7}{4}\right) f \phi' - \mathrm{Sc}\, \lambda f' \phi = 0, \tag{12}$$

subject to the boundary conditions

$$f = 0, \qquad f' = 0, \qquad \theta = \phi = 1 \quad \text{on } \eta = 0,$$

$$f' = 0, \qquad \theta = 0, \qquad \phi = 0 \quad \text{on } \eta \to \infty. \tag{13}$$

The parameters of primary interest are the Dufour number D_f, the Soret number S_r, the concentration buoyancy parameter N_1, the Prandtl number Pr, the Schmidt number Sc and the porous medium parameter Λ where

$$D_f = \frac{Dk}{c_s c_p} \frac{C_w - C_\infty}{T_w - T_\infty}, \qquad S_r = \frac{Dk}{c_s c_p} \frac{T_w - T_\infty}{C_w - C_\infty}, \qquad N_1 = \frac{\beta^*}{\beta} \frac{C_w - C_\infty}{T_w - T_\infty},$$

$$\Pr = \frac{\nu}{\alpha}, \qquad \mathrm{Sc} = \frac{\nu}{D}, \qquad \Lambda = \frac{1}{Da Gr_x^{\frac{1}{2}}}.$$

The local Nusselt and Sherwood numbers are given by the expressions

$$Nu_x = -Gr_x^{\frac{1}{4}} \theta'(0) \quad \text{and} \quad Sh_x = -Gr_x^{\frac{1}{4}} \phi'(0). \tag{14}$$

3. Method of solution

Eqs. (10)–(12) were solved first using a shooting technique with a sixth order Runge–Kutta method. For an independent verification and validation of the results a linearisation method (see [27–29]) is used to solve Eqs. (10)–(12). Below we outline the essential steps in the implementation of the successive linearisation method (SLM). We assume that the independent variables $f(\eta)$, $\theta(\eta)$ and $\phi(\eta)$ may be expanded as

$$f(\eta) = f_i(\eta) + \sum_{n=0}^{i-1} f_n(\eta), \qquad \theta(\eta) = \theta_i(\eta) + \sum_{n=0}^{i-1} \theta_n(\eta),$$

$$\phi(\eta) = \phi_i(\eta) + \sum_{n=0}^{i-1} \phi_n(\eta), \tag{15}$$

where f_i, θ_i, ϕ_i $(i = 1, 2, 3, \ldots)$ are unknown functions and f_n, θ_n and ϕ_n $(n \geq 1)$ are approximations which are obtained by recursively solving the linear part of the equation system that results from substituting Eq. (15) in Eqs. (10)–(12). Nonlinear terms in f_i, θ_i, ϕ_i and their corresponding derivatives are considered to be very small. The initial guesses $f_0(\eta)$, $\phi_0(\eta)$, $\theta_0(\eta)$

are taken to be,

$$f_0(\eta) = \frac{1}{2} + \frac{1}{2}e^{-2\eta} - e^{-\eta}, \qquad \phi_0(\eta) = e^{-\eta} \quad \text{and} \quad \theta_0(\eta) = e^{-\eta}. \tag{16}$$

These initial approximations are chosen to satisfy boundary conditions (13). The subsequent solutions for f_i, h_i, θ_i $i \geq 1$ are obtained by successively solving the linearised form of the equations which are obtained by substituting Eq. (15) in the governing equations. The linearised equations to be solved are

$$f_i''' + a_{1,i-1}f_i'' + a_{2,i-1}f_i' + a_{3,i-1}f_i + \theta_i + a_{4,i-1}\phi_i = r_{1,i-1}, \tag{17}$$

$$\theta_i'' + D_f\phi_i'' + b_{1,i-1}\theta_i' + b_{2,i-1}\theta_i + b_{3,i-1}f_i' + b_{4,i-1}f_i = r_{2,i-1}, \tag{18}$$

$$\phi_i'' + S_r\theta_i'' + c_{1,i-1}\phi_i' + c_{2,i-1}\phi_i + c_{3,i-1}f_i' + c_{4,i-1}f_i = r_{3,i-1}, \quad \text{for } i = 1, 2, 3, \ldots, \tag{19}$$

subject to the boundary conditions

$$f_i(0) = f_i'(0) = f_i'(\infty) = 0, \qquad \theta_i(0) = \theta_i(\infty) = \phi_i(0) = \phi_i(\infty) = 0. \tag{20}$$

The coefficient parameters $a_{k,i-1}, b_{k,i-1}, c_{k,i-1}$ $(k = 1, 2, 3, 4)$, $r_{j,i-1}$ $(j = 1, 2, 3)$ are defined as,

$$a_{1,i-1} = \left(\frac{\lambda+7}{4}\right)\sum_{n=0}^{i-1} f_n, \qquad a_{2,i-1} = -(\lambda+1)\sum_{n=0}^{i-1} f_n' - \Lambda, \qquad a_{3,i-1} = \left(\frac{\lambda+7}{4}\right)\sum_{n=0}^{i-1} f_n'',$$

$$a_{4,i-1} = N_1 \tag{21}$$

$$b_{1,i-1} = \mathrm{Pr}\left(\frac{\lambda+7}{4}\right)\sum_{n=0}^{i-1} f_n, \qquad b_{2,i-1} = -\mathrm{Pr}\,\lambda\sum_{n=0}^{i-1} f_n', \qquad b_{3,i-1} = -\mathrm{Pr}\,\lambda\sum_{n=0}^{i-1}\theta_n, \tag{22}$$

$$b_{4,i-1} = -\mathrm{Pr}\left(\frac{\lambda+7}{4}\right)\sum_{n=0}^{i-1}\theta_n'$$

$$c_{1,i-1} = \mathrm{Sc}\left(\frac{\lambda+7}{4}\right)\sum_{n=0}^{i-1} f_n, \qquad c_{2,i-1} = -\mathrm{Sc}\,\lambda\sum_{n=0}^{i-1} f_n', \qquad c_{3,i-1} = -\mathrm{Sc}\,\lambda\sum_{n=0}^{i-1}\phi_n, \tag{23}$$

$$c_{4,i-1} = -\mathrm{Sc}\left(\frac{\lambda+7}{4}\right)\sum_{n=0}^{i-1}\phi_n',$$

$$r_{1,i-1} = \left(\frac{\lambda+7}{2}\right)\sum_{n=0}^{i-1} f_n'\sum_{n=0}^{i-1} f_n' + \Lambda\sum_{n=0}^{i-1} f_n' - \sum_{n=0}^{i-1} f_n''' - \left(\frac{\lambda+7}{4}\right)\sum_{n=0}^{i-1} f_n\sum_{n=0}^{i-1} f_n'' - \sum_{n=0}^{i-1}\theta_n - N_1\sum_{n=0}^{i-1}\phi_n, \tag{24}$$

$$r_{2,i-1} = \mathrm{Pr}\,\lambda\sum_{n=0}^{i-1} f_n'\sum_{n=0}^{i-1}\theta_n - \sum_{n=0}^{i-1}\theta_n'' - D_f\sum_{n=0}^{i-1}\phi_n'' - \mathrm{Pr}\left(\frac{\lambda+7}{4}\right)\sum_{n=0}^{i-1} f_n'\sum_{n=0}^{i-1}\theta_n, \tag{25}$$

$$r_{3,i-1} = \mathrm{Sc}\,\lambda\sum_{n=0}^{i-1} f_n'\sum_{n=0}^{i-1}\phi_n - \sum_{n=0}^{i-1}\phi_n'' - S_r\sum_{n=0}^{i-1}\theta_n'' - \mathrm{Sc}\left(\frac{\lambda+7}{4}\right)\sum_{n=0}^{i-1} f_n'\sum_{n=0}^{i-1}\phi_n. \tag{26}$$

The solutions for f_i, θ_i, ϕ_i $(i \geq 1)$ are obtained by iteratively solving Eqs. (17)–(20). The approximate solutions for $f(\eta)$, $\theta(\eta)$ and $\phi(\eta)$ are then obtained as

$$f(\eta) \approx \sum_{m=0}^{M} f_m(\eta), \qquad \theta(\eta) \approx \sum_{m=0}^{M}\theta_m(\eta), \qquad \phi(\eta) \approx \sum_{m=0}^{M}\phi_m(\eta), \tag{27}$$

where M is the order of SLM approximation. Eqs. (17)–(20) were solved using the Chebyshev spectral collocation method. The unknown functions are approximated by the Chebyshev interpolating polynomials in such a way that they are collocated at the Gauss–Lobatto points defined as

$$\xi_j = \cos\frac{\pi j}{N}, \quad j = 0, 1, \ldots, N \tag{28}$$

where N is the number of collocation points used. The physical region $[0, \infty)$ is transformed into the region $[-1, 1]$ using the domain truncation technique in which the problem is solved on the interval $[0, L]$ instead of $[0, \infty)$. This leads to the mapping

$$\frac{\eta}{L} = \frac{\xi+1}{2}, \quad -1 \leq \xi \leq 1 \tag{29}$$

where L is the scaling parameter used to invoke the boundary condition at infinity. The functions f_i, θ_i and ϕ_i are approximated at the collocation points by

$$f_i(\xi) \approx \sum_{k=0}^{N} f_i(\xi_k) T_k(\xi_j), \qquad \theta_i(\xi) \approx \sum_{k=0}^{N} \theta_i(\xi_k) T_k(\xi_j), \qquad \phi_i(\xi) \approx \sum_{k=0}^{N} \phi_i(\xi_k) T_k(\xi_j), \quad j = 0, 1, \ldots, N \tag{30}$$

where T_k is the kth Chebyshev polynomial defined as

$$T_k(\xi) = \cos[k \cos^{-1}(\xi)]. \tag{31}$$

The derivatives of the variables at the collocation points are represented as

$$\frac{d^a f_i}{d\eta^a} = \sum_{k=0}^{N} \mathbf{D}_{kj}^a f_i(\xi_k), \qquad \frac{d^a \theta_i}{d\eta^a} = \sum_{k=0}^{N} \mathbf{D}_{kj}^a \theta_i(\xi_k), \qquad \frac{d^a \phi_i}{d\eta^a} = \sum_{k=0}^{N} \mathbf{D}_{kj}^a \phi_i(\xi_k), \quad j = 0, 1, \ldots, N \tag{32}$$

where a is the order of differentiation and $\mathbf{D} = \frac{2}{L}\mathcal{D}$ with $\mathcal{D}$ being the Chebyshev spectral differentiation matrix. Substituting Eqs. (29)–(32) into Eqs. (17)–(20) leads to the matrix equation

$$\mathbf{A}_{i-1}\mathbf{X}_i = \mathbf{R}_{i-1}, \tag{33}$$

subject to the boundary conditions

$$f_i(\xi_N) = 0, \qquad \sum_{k=0}^{N} \mathbf{D}_{Nk} f_i(\xi_k) = 0, \qquad \sum_{k=0}^{N} \mathbf{D}_{0k} f_i(\xi_k) = 0 \tag{34}$$

$$\theta_i(\xi_N) = \theta_i(\xi_0) = \phi_i(\xi_N) = \phi_i(\xi_0) = 0. \tag{35}$$

In Eq. (33), $\mathbf{A}_{i-1}$ is a $(3N+3) \times (3N+3)$ square matrix and $\mathbf{X}_i$ and $\mathbf{R}_i$ are $(3N+1) \times 1$ column vectors defined by

$$\mathbf{A}_{i-1} = \begin{bmatrix} A_{11} & A_{12} & A_{13} \\ A_{21} & A_{22} & A_{23} \\ A_{31} & A_{32} & A_{33} \end{bmatrix}, \qquad \mathbf{X}_i = \begin{bmatrix} \mathbf{F}_i \\ \mathbf{\Theta}_i \\ \mathbf{\Phi}_i \end{bmatrix}, \qquad \mathbf{R}_{i-1} = \begin{bmatrix} \mathbf{r}_{1,i-1} \\ \mathbf{r}_{2,i-1} \\ \mathbf{r}_{3,i-1} \end{bmatrix}, \tag{36}$$

where

$$\mathbf{F}_i = [f_i(\xi_0), f_i(\xi_1), \ldots, f_i(\xi_{N-1}), f_i(\xi_N)]^T, \tag{37}$$

$$\mathbf{\Theta}_i = [\theta_i(\xi_0), \theta_i(\xi_1), \ldots, \theta_i(\xi_{N-1}), \theta_i(\xi_N)]^T, \tag{38}$$

$$\mathbf{\Phi}_i = [\phi_i(\xi_0), \phi_i(\xi_1), \ldots, \phi_i(\xi_{N-1}), \phi_i(\xi_N)]^T, \tag{39}$$

$$\mathbf{r}_{1,i-1} = [r_{1,i-1}(\xi_0), r_{1,i-1}(\xi_1), \ldots, r_{1,i-1}(\xi_{N-1}), r_{1,i-1}(\xi_N)]^T, \tag{40}$$

$$\mathbf{r}_{2,i-1} = [r_{2,i-1}(\xi_0), r_{2,i-1}(\xi_1), \ldots, r_{2,i-1}(\xi_{N-1}), r_{2,i-1}(\xi_N)]^T, \tag{41}$$

$$\mathbf{r}_{3,i-1} = [r_{3,i-1}(\xi_0), r_{3,i-1}(\xi_1), \ldots, r_{3,i-1}(\xi_{N-1}), r_{3,i-1}(\xi_N)]^T, \tag{42}$$

$$A_{11} = \mathbf{D}^3 + \mathbf{a}_{1,i-1}\mathbf{D}^2 + \mathbf{a}_{2,i-1}\mathbf{D} + \mathbf{a}_{3,i-1}\mathbf{I}, \qquad A_{12} = \mathbf{I}, \qquad A_{13} = \mathbf{a}_{4,i-1}\mathbf{I} \tag{43}$$

$$A_{21} = \mathbf{b}_{3,i-1}\mathbf{D} + \mathbf{b}_{4,i-1}\mathbf{I}, \qquad A_{22} = \mathbf{D}^2 + \mathbf{b}_{1,i-1}\mathbf{D} + \mathbf{b}_{2,i-1}\mathbf{I}, \qquad A_{23} = D_f\mathbf{D}^2, \tag{44}$$

$$A_{31} = \mathbf{c}_{3,i-1}\mathbf{D} + \mathbf{c}_{4,i-1}\mathbf{I}, \qquad A_{32} = S_r\mathbf{D}^2, \qquad A_{33} = \mathbf{D}^2 + \mathbf{c}_{1,i-1}\mathbf{D} + \mathbf{c}_{2,i-1}\mathbf{I}. \tag{45}$$

In the above definitions, $\mathbf{a}_{k,i-1}$, $\mathbf{b}_{k,i-1}$, $\mathbf{c}_{k,i-1}$ $(k = 1, 2, 3, 4)$ are diagonal matrices of size $(N+1) \times (N+1)$ and $\mathbf{I}$ is an identity matrix of size $(N+1) \times (N+1)$. After modifying the matrix system (33) to incorporate boundary conditions (34)–(35), the solution is obtained as

$$\mathbf{X}_i = \mathbf{A}_{i-1}^{-1}\mathbf{R}_{i-1}. \tag{46}$$

4. Results and discussions

The results showing the effects of various parameters on the skin-friction coefficient, the local heat and mass transfer rates on flow surrounding an inverted cone in a porous medium are given in Tables 1–6. The results at different orders of the successive linearisation method (SLM), the in-built Matlab bvp4c routine and the sixth order Runge–Kutta method are given side-by-side firstly to give a sense of the convergence rate of the successive linearisation method, and secondly, to show the accuracy of the results in this study. In general, the SLM has converged to the numerical results by the sixth or seventh order. In this study we have used $\mathrm{Pr} = 0.71$ which corresponds to air at about 20 °C.

Table 1
Effect of porous medium parameter Λ on skin-friction, heat and mass transfer coefficients when $\mathrm{Sc} = 0.2$, $N_1 = 0.5$, $D_f = 0.1$, $S_r = 0.3$ and $\lambda = 1$.

	Λ	SLM			bvp4c	RK6
		Order 1	Order 7	Order 8		
$f''(0)$	0.0	1.1843470	1.0867503	1.0867503	1.0867503	1.0867503
	0.1	1.1425882	1.0619211	1.0619211	1.0619211	1.0619211
	0.3	1.0765266	1.0160906	1.0160906	1.0160906	1.0160906
	0.5	1.0228513	0.9748755	0.9748755	0.9748755	0.9748755
$Nu_x/Gr_x^{\frac{1}{4}}$	0.0	0.7910581	0.6775009	0.6775009	0.6775009	0.6775009
	0.1	0.7563635	0.6687416	0.6687416	0.6687416	0.6687416
	0.3	0.7098302	0.6519703	0.6519703	0.6519703	0.6519703
	0.5	0.6760873	0.6361752	0.6361752	0.6361752	0.6361752
$Sh_x/Gr_x^{\frac{1}{4}}$	0.0	0.1509866	0.2378137	0.2378137	0.2378137	0.2378137
	0.1	0.1449825	0.2334291	0.2334291	0.2334291	0.2334291
	0.3	0.1373305	0.2250080	0.2250080	0.2250080	0.2250080
	0.5	0.1320026	0.2170624	0.2170624	0.2170624	0.2170624

Table 2
Effect of Schmidt number Sc on skin-friction, heat and mass transfer coefficients when $\Lambda = 0.5$, $N_1 = 0.5$, $D_f = 0.1$, $S_r = 0.3$ and $\lambda = 1$.

	Sc	SLM			bvp4c	RK6
		Order 1	Order 5	Order 6		
$f''(0)$	0.2	1.0228513	0.9748759	0.9748755	0.9748755	0.9748755
	0.3	0.9958299	0.9556299	0.9556299	0.9556299	0.9556299
	0.4	0.9760609	0.9416563	0.9416563	0.9416563	0.9416563
	0.5	0.9607540	0.9307654	0.9307654	0.9307654	0.9307654
$Nu_x/Gr_x^{\frac{1}{4}}$	0.2	0.6760873	0.6361758	0.6361752	0.6361752	0.6361752
	0.3	0.6420774	0.6191770	0.6191770	0.6191770	0.6191770
	0.4	0.6184924	0.6060929	0.6060929	0.6060929	0.6060929
	0.5	0.6009331	0.5954969	0.5954969	0.5954969	0.5954969
$Sh_x/Gr_x^{\frac{1}{4}}$	0.2	0.1320026	0.2170619	0.2170624	0.2170624	0.2170624
	0.3	0.2379864	0.3008282	0.3008282	0.3008282	0.3008282
	0.4	0.3219282	0.3684395	0.3684395	0.3684395	0.3684395
	0.5	0.3917392	0.4257367	0.4257367	0.4257367	0.4257367

Table 3
Effect of buoyancy parameter on skin-friction, heat and mass transfer coefficients when $\lambda = 1$, $\Lambda = 0.5$, $D_f = 0.1$, $S_r = 0.3$ and $\mathrm{Sc} = 0.2$.

	N_1	SLM				bvp4c	RK6
		Order 3	Order 4	Order 5	Order 6		
$f''(0)$	0.1	0.7166291	0.7166208	0.7166208	0.7166208	0.7166208	0.7166208
	0.3	0.8480853	0.8480336	0.8480329	0.8480329	0.8480329	0.8480329
	0.7	1.0978920	1.0977198	1.0977125	1.0977125	1.0977125	1.0977125
	1.3	1.4473863	1.4470978	1.4470857	1.4470856	1.4470855	1.4470855
$Nu_x/Gr_x^{\frac{1}{4}}$	0.1	0.5534005	0.5533681	0.5533681	0.5533681	0.5533680	0.5533680
	0.3	0.5992846	0.5988793	0.5988735	0.5988735	0.5988735	0.5988735
	0.7	0.6704941	0.6682603	0.6681653	0.6681649	0.6681649	0.6681649
	1.3	0.7513607	0.7451900	0.7448083	0.7448051	0.7448051	0.7448051
$Sh_x/Gr_x^{\frac{1}{4}}$	0.1	0.1726641	0.1728297	0.1728300	0.1728300	0.1728300	0.1728300
	0.3	0.1978456	0.1985334	0.1985432	0.1985432	0.1985432	0.1985432
	0.7	0.2304610	0.2319248	0.2319774	0.2319776	0.2319776	0.2319776
	1.3	0.2632016	0.2653895	0.2654867	0.2654872	0.2654872	0.2654872

Table 1 shows the effect of permeability parameter Λ on the skin-friction, the heat and the mass transfer coefficients. Firstly we note a remarkable agreement between the numerical and the linearisation results, and secondly, as the permeability increases, the skin-friction coefficient, the local Nusselt number and the local Sherwood number all decrease. In an earlier study on heat transfer in a porous medium over a stretching surface, Sultana et al. [30] also found that both the skin-friction coefficient and the rate of heat transfer decreases with increasing permeability.

Table 2 shows that while the skin-friction coefficient and the local Nusselt number decrease with Schmidt numbers. However, the rate of mass transfer increases with Sc.

Table 3 illustrates the effects of buoyancy parameter N_1 on the shear stress $f''(0)$ between the fluid flow and the cone surface, the Nusselt number and the Sherwood number. Increasing fluid buoyancy enhances the wall shear stress and the local heat and mass transfer rates; see Mahdy [31].

Table 4
Effect of λ on the skin-friction, heat and mass transfer coefficients when $N_1 = 0.5$, $\Lambda = 0.5$, $D_f = 0.1$, $S_r = 0.3$ and Sc $= 0.2$.

	λ	SLM				bvp4c	RK6
		Order 3	Order 4	Order 5	Order 6		
$f''(0)$	0.0	1.0861428	1.0858029	1.0857945	1.0857945	1.0857945	1.0857945
	0.3	1.0460083	1.0457695	1.0457628	1.0457628	1.0457628	1.0457628
	0.6	1.0124024	1.0122310	1.0122259	1.0122259	1.0122259	1.0122259
	1.0	0.9749785	0.9748655	0.9748621	0.9748621	0.9748621	0.9748621
$Nu_x/Gr_x^{\frac{1}{4}}$	0.0	0.5082375	0.5064365	0.5063663	0.5063661	0.5063661	0.5063661
	0.3	0.5541051	0.5524765	0.5524179	0.5524177	0.5524177	0.5524177
	0.6	0.5930703	0.5916358	0.5915882	0.5915881	0.5915881	0.5915881
	1.0	0.6373816	0.6361986	0.6361636	0.6361635	0.6361635	0.6361635
$Sh_x/Gr_x^{\frac{1}{4}}$	0.0	0.1582770	0.1598337	0.1598900	0.1598901	0.1598901	0.1598901
	0.3	0.1783143	0.1797883	0.1798383	0.1798384	0.1798384	0.1798384
	0.6	0.1957612	0.1970983	0.1971399	0.1971400	0.1971400	0.1971400
	1.0	0.2159151	0.2170453	0.2170762	0.2170763	0.2170763	0.2170763

Table 5
Effect of Dufour parameter on the skin-friction, heat and mass transfer coefficients when $N_1 = 0.5$, $\Lambda = 0.5$, $\lambda = 1$, $S_r = 0.3$ and Sc $= 0.2$.

	D_f	SLM				bvp4c	RK6
		Order 3	Order 4	Order 5	Order 6		
$f''(0)$	0.0	0.9726550	0.9725516	0.9725488	0.9725488	0.9725488	0.9725488
	0.8	0.9921930	0.9919858	0.9919775	0.9919775	0.9919775	0.9919775
	1.6	1.0142892	1.0138913	1.0138788	1.0138789	1.0138788	1.0138788
	2.4	1.0400075	1.0392891	1.0392765	1.0392767	1.0392767	1.0392767
$Nu_x/Gr_x^{\frac{1}{4}}$	0.0	0.6406844	0.6395961	0.6395664	0.6395664	0.6395663	0.6395663
	0.8	0.6118610	0.6100432	0.6099662	0.6099659	0.6099659	0.6099659
	1.6	0.5758196	0.5733909	0.5732633	0.5732625	0.5732625	0.5732625
	2.4	0.5284654	0.5257015	0.5255273	0.5255256	0.5255256	0.5255256
$Sh_x/Gr_x^{\frac{1}{4}}$	0.0	0.2133998	0.2145092	0.2145382	0.2145383	0.2145383	0.2145383
	0.8	0.2328248	0.2338522	0.2338735	0.2338735	0.2338735	0.2338735
	1.6	0.2520662	0.2526126	0.2525795	0.2525789	0.2525789	0.2525789
	2.4	0.2730172	0.2728306	0.2727220	0.2727203	0.2727203	0.2727203

Table 6
Effect of Soret parameter on the skin-friction, heat and mass transfer coefficients when $N_1 = \Lambda = 0.5$, $\lambda = 1$, $D_f = 0.1$ and Sc $= 0.2$.

	S_r	SLM				bvp4c	RK6
		Order 3	Order 4	Order 5	Order 6		
$f''(0)$	0.0	0.9536355	0.9535874	0.9535864	0.9535864	0.9535864	0.9535864
	0.3	0.9749785	0.9748655	0.9748621	0.9748621	0.9748621	0.9748621
	0.6	0.9967960	0.9965740	0.9965665	0.9965665	0.9965665	0.9965665
	1.0	1.0266695	1.0261899	1.0261745	1.0261744	1.0261744	1.0261744
$Nu_x/Gr_x^{\frac{1}{4}}$	0.0	0.6180131	0.6174916	0.6174825	0.6174825	0.6174825	0.6174825
	0.3	0.6373816	0.6361986	0.6361636	0.6361635	0.6361635	0.6361635
	0.6	0.6567077	0.6545804	0.6544950	0.6544947	0.6544947	0.6544947
	1.0	0.6828206	0.6789484	0.6787524	0.6787514	0.6787514	0.6787514
$Sh_x/Gr_x^{\frac{1}{4}}$	0.0	0.3311003	0.3315570	0.3315650	0.3315651	0.3315650	0.3315650
	0.3	0.2159151	0.2170453	0.2170762	0.2170763	0.2170763	0.2170763
	0.6	0.0936177	0.0958684	0.0959467	0.0959469	0.0959469	0.0959469
	1.0	0.0814522	0.0766974	0.0764993	0.0764985	0.0764985	0.0764985

In this study the power-law index was varied in the range $0 \leq \lambda \leq 1$, that is, the ambient temperature and concentration varied from a constant to a linear function of the distance along the cone surface. Table 4 shows that increasing λ reduces the skin friction, but enhances the rates of heat and mass transfer. Nield and Bejan [3] reported the same result for the thermal coefficient.

Table 5 shows the effect of Dufour number D_f on the wall stress, the local Nusselt number and the local Sherwood number. Increasing the Dufour number enhances the skin-friction coefficient and mass transfer but reduces the local heat transfer rate. The same result has been reported by Islam and Alam [32] for free convection in a rotating system.

The effect of Soret number S_r on the skin-friction coefficient, the heat and the mass transfer rates is shown in Table 6. It is clear that $f''(0)$ and Nu_x increase with S_r but that the local mass transfer rate decreases as S_r increases. A similar finding has been reported by Partha [33] for a vertical plate embedded in a non-Darcy porous medium.

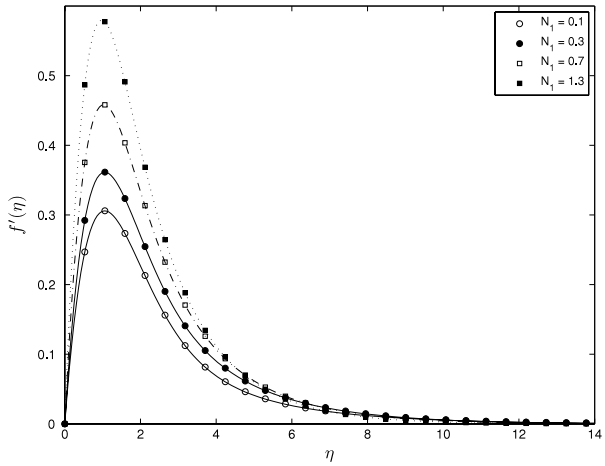

Fig. 2. Effect of buoyancy parameter on the velocity profiles when $\lambda = 1$, $\Lambda = 0.5$, $S_r = 0.3$, $D_f = 0.1$ and Sc $= 0.2$.

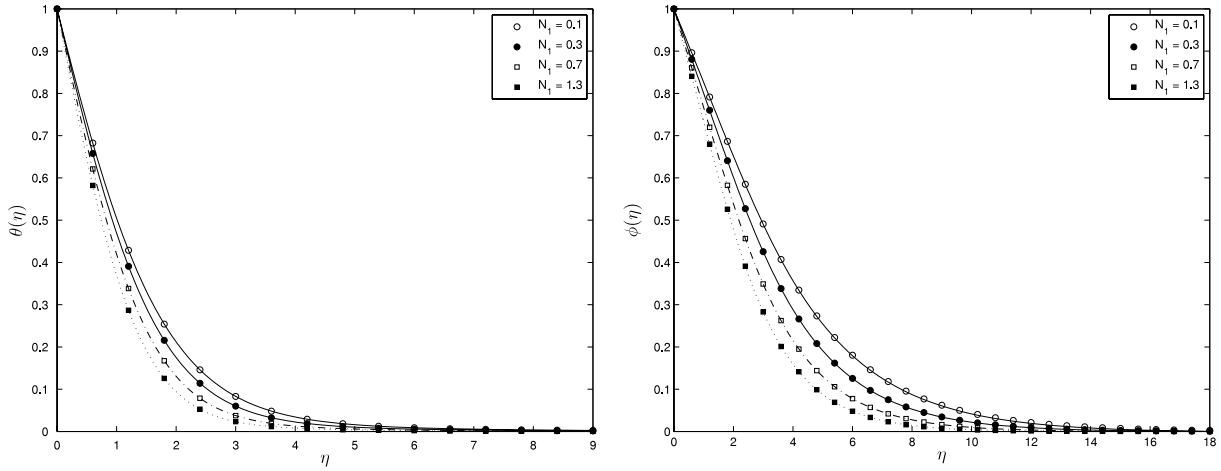

Fig. 3. Effect of buoyancy parameter on the temperature and the concentration profiles when $\lambda = 1$, $\Lambda = 0.5$, $S_r = 0.3$, $D_f = 0.1$ and Sc $= 0.2$.

Figs. 2–9 serve a dual purpose; to give a comparison of the accuracy of the numerical and the SLM results as well as to demonstrate the effect of various parameters on the velocity, temperature and concentration profiles. The circles and triangles represent the SLM solution. Fig. 2 shows the effects of buoyancy parameter on the velocity profile. With an increase in fluid buoyancy the velocity increases.

Fig. 3 displays the temperature and the concentration profiles for various values of the buoyancy parameter. Increasing buoyancy tends to reduce the temperature and the concentration profiles.

The effect of power-law index λ on the velocity, temperature and the concentration profiles is shown in Figs. 4 and 5. The velocity peaks at higher levels when the ambient temperature and concentration is constant and reduces with λ. The temperature and the concentration profiles decrease with increasing λ. Fig. 6 shows the effect of Dufour number on the temperature profiles. As the Dufour parameter increases, the thermal thickness decreases, thus increasing the heat transfer rate at the wall.

Fig. 7 shows the effects of Soret parameter S_r on concentration profile. Increasing S_r leads to increase in concentration thickness of the boundary layer; in other words, there is increase in mass transfer at the cone wall. Figs. 8 and 9 show the effect of medium porosity on the velocity, temperature and concentration profiles. The velocity decreases with increasing porosity, while both the temperature and concentration profiles thicken with increasing medium porosity.

5. Conclusions

In this paper we have studied the effects of cross-diffusion on the skin-friction coefficient, the heat and the mass transfer from an inverted cone in a porous medium. Numerical solutions for the governing momentum, energy and concentration equations were found using a shooting method together with a sixth order Runge–Kutta method. The results were validated by using a linearisation method. Tabulated and graphical results were presented showing the effect of various fluid and

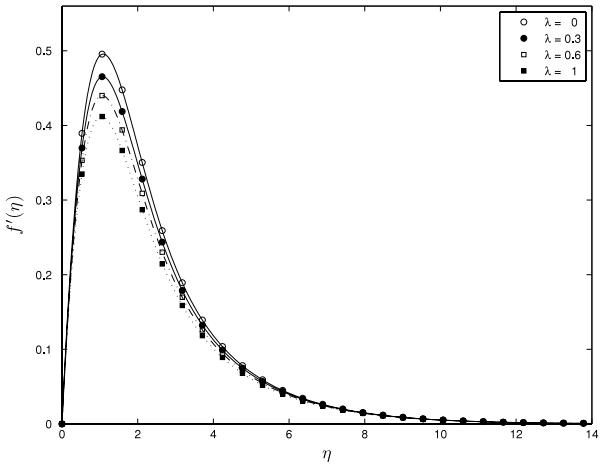

Fig. 4. Effect of λ on the velocity profiles when $N_1 = 0.5$, $\Lambda = 0.5$, $S_r = 0.3$, $D_f = 0.1$ and Sc $= 0.2$.

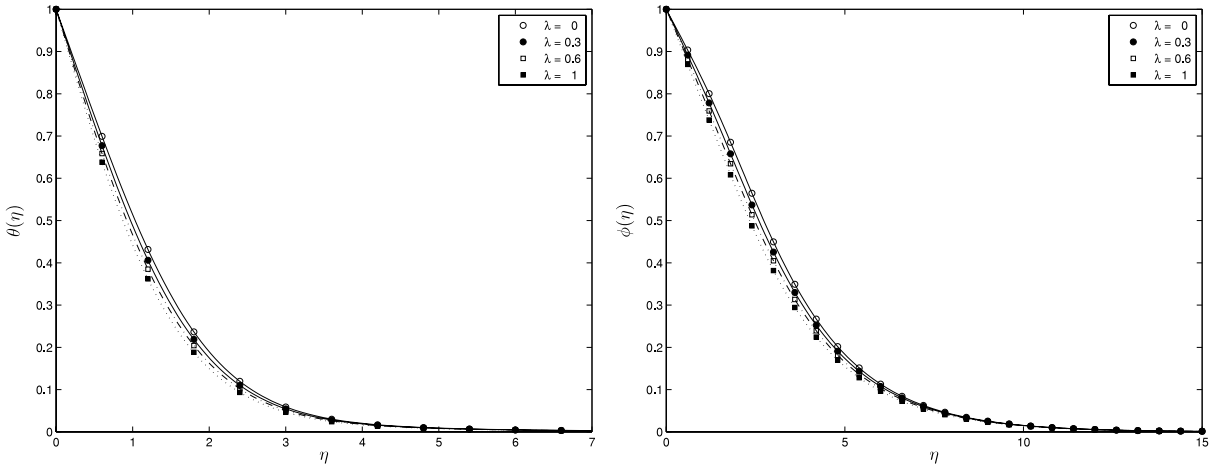

Fig. 5. Effect of λ on the temperature and the concentration profiles when $N_1 = \Lambda = 0.5$, $S_r = 0.3$, $D_f = 0.1$ and Sc $= 0.2$.

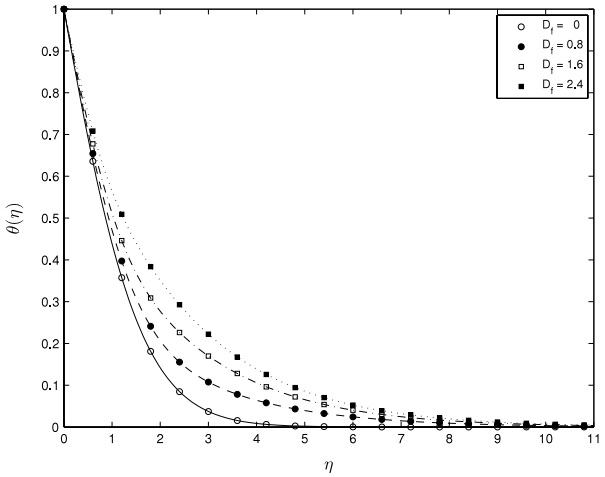

Fig. 6. Effect of Dufour parameter D_f on the temperature profile when $\lambda = 1$, $N_1 = \Lambda = 0.5$, $S_r = 0.3$ and Sc $= 0.2$.

medium parameters on velocity, thermal and concentration profiles as well as on the skin-friction coefficient, the heat and the mass transfer rates. From the present study we can see that the stronger buoyancy leads to higher velocity, whereas both

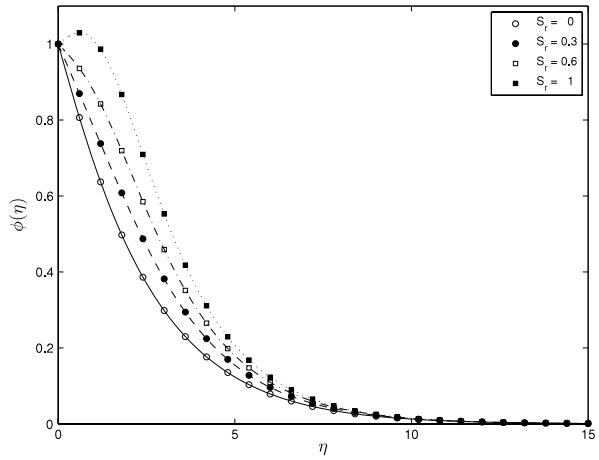

Fig. 7. Effect of Soret parameter S_r on the concentration profiles when $\lambda = 1$, $N_1 = \Lambda = 0.5$, $D_f = 0.1$ and Sc $= 0.2$.

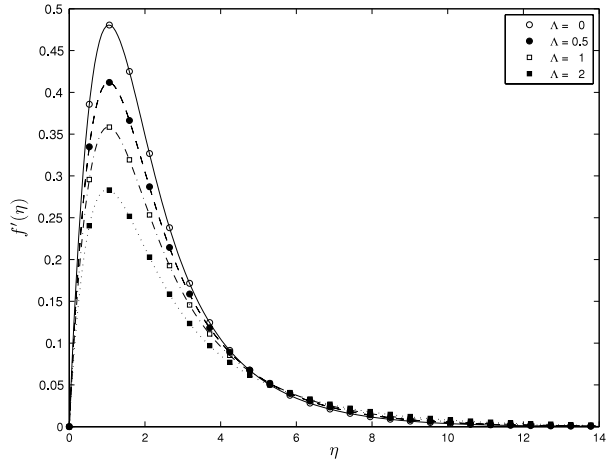

Fig. 8. Effect of porosity parameter on the velocity profiles when $\lambda = 1$, $N_1 = 0.5$, $S_r = 0.3$, $D_f = 0.1$ and $\Lambda = 0.5$.

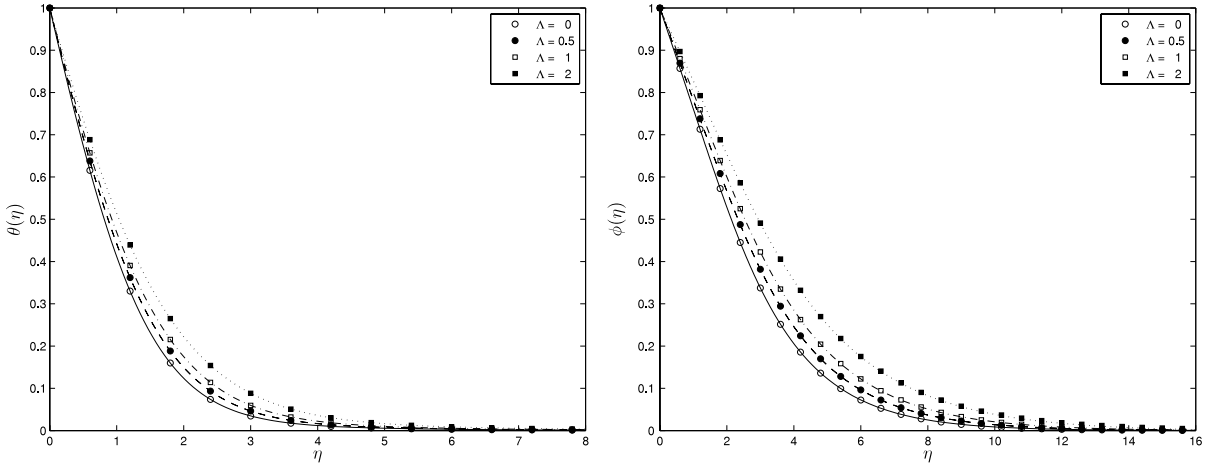

Fig. 9. Effect of porosity parameter on the temperature and the concentration profiles when $\lambda = 1$, $N_1 = 0.5$, $S_r = 0.3$, $D_f = 0.1$ and $\Lambda = 0.2$.

the thermal and concentration thickness of the boundary layer decrease. The thermal and the concentration of the boundary layer decrease as the power-law index λ increases. The mass transfer increases with increase in the Soret parameter. Increasing the Dufour parameter leads to a decrease in the thermal thickness of the boundary layer.

References

[1] P. Cheng, Similarity solutions for mixed convection from horizontal impermeable surfaces in saturated porous media, International Journal of Heat Mass Transfer (9) (1977) 893–898.
[2] P. Cheng, Natural convection in a porous medium: external flow, in: Proceedings of the NATO Advanced Study in Natural Convection, Ezmir, Turkey, 1985.
[3] D.A. Nield, A. Bejan, Convection in Porous Media, 2nd ed., Springer-Verlag, New York, 1999.
[4] I. Pop, D.B. Ingham, Convective Heat Transfer, 1st ed., Elsevier, 2001.
[5] T.Y. Na, J.P. Chiou, Laminar natural convection over a frustum of a cone, Applied Scientific Research 35 (1979) 409–421.
[6] F.C. Lai, Coupled heat and mass transfer by natural convection from a horizontal line source in saturated porous medium, International Communications in Heat and Mass Transfer 17 (1990) 489–499.
[7] I. Pop, T.Y. Na, Natural convection of a Darcian fluid about a cone, International Communications in Heat and Mass Transfer 12 (1994) 891–899.
[8] A. Nakayama, M.A. Hossain, An integral treatment for combined heat and mass transfer by natural convection in a porous medium, International Journal of Heat Mass Transfer 38 (1995) 761–765.
[9] C.Y. Cheng, Effect of a magnetic field on heat andmass transfer by natural convection from vertical surfaces in porous media — an integral approach, International Communications in Heat and Mass Transfer 26 (1999) 935–943.
[10] A.J. Chamkha, A.A. Khaled, Nonsimilar hydromagnetic simultaneous heat and mass transfer by mixed convection from a vertical plate embedded in a uniform porous medium, Numerical Heat Transfer Part A: Applications 36 (1999) 327–344.
[11] A.J. Chamkha, Coupled heat and mass transfer by natrual convection about a truncated cone in the presence of magnetic field and radiation effects, Numerical Heat Transfer Part A: Applications 39 (2001) 511–530.
[12] K.A. Yih, Coubled heat and mass transfer by free convecton over a truncated cone in porous media: VWT/VWC or VHF/VMF, Acta Mechanica 137 (1999) 83–97.
[13] C.Y. Cheng, An integral approach for heat and mass transfer by natural convection from truncated cones in porous media with variable wall temperature and concentration, International Communications in Heat and Mass Transfer 27 (2000) 437–548.
[14] C.Y. Cheng, Soret and Dufour effects on natural convection heat and mass transfer from a vertical cone in a porous medium, International Communications in Heat and Mass Transfer 36 (2009) 1020–1024.
[15] K. Khanafer, K. Vafai, Double-diffusive mixed convection in a lid-driven enclosure filled with a fluid-saturated porous medium, Numerical Heat Transfer Part A: Applications 42 (2002) 465–486.
[16] B.V. Rathish Kumar, P. Singh, V.J. Bansod, Effect of thermal stratification on doublediffusive natural convection in a vertical porous enclosure, Numerical Heat Transfer Part A: Applications 41 (2002) 421–447.
[17] A.T. Atimtay, W.N. Gill, The effect of free stream concentration on heat and binary mass transfer with thermodynamic coupling in convection on a rotating disc, Chemical Engineering Communications 34 (1985) 161–185.
[18] D.E. Rosner, Thermal (Soret) diffusion effects on interfacial mass transport rates, PhysicoChemical Hydrodynamics 1 (1980) 159–185.
[19] X. Yu, Z. Guo, B. Shi, Numerical study of cross-diffusion effects on double diffusive convection with lattice Boltzmann method, in: Shi, et al. (Eds.), ICCS, in: LNCS, vol. 4487, Springer-Verlag, Berlin, 2007, pp. 810–817.
[20] N.G. Kafoussias, E.M. Williams, Thermal-diffusion and diffusion-thermo effects on mixed free-forced convective and mass transfer boundary layer flow with temperature dependent viscosity, International Journal of Engineering Science 33 (1995) 1369–1384.
[21] A.J. Chamkha, A. Ben-Nakhi, MHD mixed convection-radiation interaction along a permeable surface immersed in a porous medium in the presence of Soret and Dufour's Effect, Heat Mass Transfer 44 (2008) 845–856.
[22] O. Sovran, M.C. Charrier-Mojtabi, A. Mojtabi, Comptes Rendus de l'Academie des Sciences, Paris 329 (2001) 287–293.
[23] A. Postelnicu, Influence of a magnetic field on heat and mass transfer by natural convection from vertical surfaces in porous media considering Soret and Dufour effects, Int. J. Heat and Mass Transfer 47 (2004) 1467–1472.
[24] A.R. Sohouli, M. Famouri, A. Kimiaeifar, G. Domairry, Application of homotopy analysis method for natural convection of Darcian fluid about a vertical full cone embedded in pours media prescribed surface heat flux, Communications in Nonlinear Science and Numerical Simulation 15 (2010) 1691–1699.
[25] S.D. Conte, C. De Boor, Elementary Numerical Analysis, McGraw-Hill, New York, 1972.
[26] T. Cebeci, P. Bradshaw, Physical and Computational Aspects of Convective Heat Transfer, Springer, New York, 1984.
[27] Z. Makukula, S.S. Motsa, P. Sibanda, On a new solution for the viscoelastic squeezing flow between two parallel plates, Journal of Advanced Research in Applied Mathematics 2 (2010) 31–38.
[28] Z.G. Makukula, P. Sibanda, S.S. Motsa, A novel numerical technique for two-dimensional laminar flow between two moving porous walls, Mathematical Problems in Engineering (2010) 15 pages. Article ID 528956. doi:10.1155/2010/528956.
[29] S. Shateyi, S.S. Motsa, Variable viscosity on magnetohydrodynamic fluid flow and heat transfer over an unsteady stretching surface with hall effect, Boundary Value Problems (2010) 20 pages. Article ID 257568. doi:10.1155/2010/257568.
[30] T. Sultana, S. Saha, M.M. Rahman, G. Saha, Heat transfer in a porous medium over a stretching surface with internal heat generation and suction or injection in the presence of radiation, Journal of Mechanical Engineering 40 (2009) 22–28.
[31] A. Mahdy, Soret and Dufour effect on double diffusion mixed convection from a vertical surface in a porous medium saturated with a non-Newtonian fluid, Journal of Non-Newtonian Fluid Mechanics 165 (2010) 568–575.
[32] N. Islam, Md.M. Alam, Dufour and Soret effects on steady MHD free convection and mass transfer fluid flow through a porous medium in a rotating system, Journal of Naval Architecture and Marine Engineering 4 (2007) 43–55.
[33] M.K. Partha, Suction/injection effects on thermophoresis particle deposition in a non-Darcy porous meduim under the influence of Soret, Dufour effects, International Journal Heat and Mass Transfer 52 (2009) 1971–1979.